Absolute dissociative electron attachment cross-section measurement of difluoromethane

Dipayan Chakraborty [1,*] and Dhananjay Nandi [1,2,†]

[1] *Indian Institute of Science Education and Research Kolkata, Mohanpur 741246, India*

[2] *Center for Atomic, Molecular and Optical Sciences & Technologies, Joint initiative of IIT Tirupati & IISER Tirupati, Yerpedu, 517619, Andhra Pradesh, India*

(Received 23 August 2020; accepted 20 October 2020; published 3 November 2020)

Dissociative electron attachment (DEA) to difluoromethane (CH_2F_2) has been studied in the electron energy range of 0 to 16 eV. Two resonant states around 2 and 11.4 eV leading to three different fragment anions (F^-, CHF^-, and $F_2{}^-$) are observed. Ion-yield curves of the negative ions help us to locate the position of the resonant states. In the ion-yield curve of F^- ions, one small hump near 9.8 eV followed by a peak around 15.2 eV is also observed. Absolute DEA cross sections of the F^- ion is measured by using the well-known relative flow technique. Dissociation channels associated with each resonant states are identified by density-functional theory (DFT) calculations of the threshold energies. The theory matches quite well within the experimental uncertainty.

DOI: 10.1103/PhysRevA.102.052801

I. INTRODUCTION

Total elastic and inelastic electron-scattering cross-section studies of fluoromethanes is a topic of interest these days [1]. Cross-section values of these molecules have demand because of its application to plasma processing in the semiconductor industry. Beside these, chlorofluorocarbons (CFCs) and hydrofluorocarbons (HFCs) are the main reason behind the ozone layer depletion due to their photolytic decomposition. However, decomposition can also occur due to the low-energy electron attachment process, named "dissociative electron attachment" (DEA) [2]. DEA is a two-step resonant process; in the first step, a low-energy electron interacts with a neutral molecule and is captured resonantly to form a temporary negative ion (TNI) state. In the second step, the TNI dissociates into a negative ion and one or more neutral conjugates. So, it is absolutely necessary to have accurate DEA cross-section values of these molecules. Several studies are performed in this direction [3–5], but for difluoromethane (CH_2F_2) it is rare. Apart from the absolute cross-section measurements, the low-energy electron attachment to halomethanes were also investigated by several groups. In 1992, Modelli *et al.* [6] studied the electron attachment to the halomethanes via electron transmission spectroscopy and observed that low-energy electrons are attached with the halomethanes, although, for fluoromethanes, they did not report any low-energy (<6 eV) resonances. In 2000 Langer *et al.* [7] measured the negative-ion formation due to low-energy electron collision to CF_2Cl_2. In this study, the authors observed a low-energy TNI state (in the ion-yield curve, the resonance peaks are observed around 0, 1.7 eV for Cl^-, 3 eV for F^-, 2.8 eV for $CFCl_2{}^-$ and ClF^-, and 1 eV for $Cl_2{}^-$) which dissociates via different fragment negative ions. They concluded that the TNI state, which dissociates via Cl^- negative-ion formation, is formed due to shape resonance, where the incoming electron occupies the molecular orbital with σ^*(C-Cl) character.

CH_2F_2 is colorless, odourless, extremely flammable, and widely used as a refrigerant (see Fig. 1). It is insoluble in water and heavier than air. The electronic structure and energy of the CH_2F_2 molecule has been studied by Brundle *et al.* [8]. Tanaka *et al.* [9] obtained elastic differential cross sections below 100 eV incident electron energy; later, the integral cross section was also calculated [10]. Nishimura [11] calculated theoretically the vibrationally elastic-scattering cross section of CH_2F_2 with electron collisions below 30 eV. All these studies were limited to only the elastic electron-scattering cross section of CH_2F_2, but the inelastic-scattering processes like dissociative ionization (DI), DEA, and ion-pair dissociation (IPD) process of CH_2F_2 were neglected. Our recent study [12] addresses both the DEA and IPD processes. In 1998, Motlagh and Moore [13] studied the electron-impact DI process of CH_2F_2 molecule up to 500 eV incident electron energy range. Later, Torres *et al.* [14] studied the same up to the 100 eV energy range by using the time-of-flight mass spectrometry method. The authors discussed in detail the appearance energy, absolute total cross section, dissociative ionization cross sections, and the corresponding kinetic energy of the fragment ions. The DEA and IPD process of the CH_2F_2 molecule was studied by Scheuremann *et al.* [15], where the authors discussed different anions and their corresponding ion-yield curves. Recently, Gao *et al.* [16] studied the DEA to CH_2F_2 molecules by using the velocity map imaging (VMI) technique, where the author focused on the formation of CHF^- anions only.

The absolute DEA cross section and complete DEA mass spectrometric studies of CH_2F_2 are not available to date. In the present study, DEA to CH_2F_2 is discussed within the 0 to 16 eV energy range, using a recently developed advanced time-of-flight mass spectrometer [17]. The absolute DEA cross section of the F^- ion is reported herein. Due to very low count rate, the absolute cross section for the other two fragments (namely, CHF^- and $F_2{}^-$) is not

*Present address: Radiation Laboratory, University of Notre Dame, Notre Dame, Indiana 46556, USA.

†dhananjay@iiserkol.ac.in

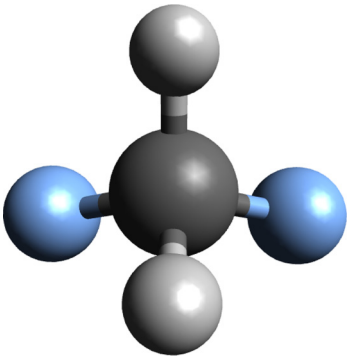

FIG. 1. Molecular structure of CH_2F_2 molecule. The two fluorine (blue color) and two hydrogen atoms are connected to the carbon atom.

reported here; the differential cross section is reported instead. Furthermore, we did not succeed to probe velocity map imaging spectrometer for meaningful measurements, again due to a very low count rate. With the help of quantum chemical calculations, threshold energies of different dissociation channels corresponding to different resonant states are calculated.

II. EXPERIMENTAL AND COMPUTATIONAL METHODS

Details of the experimental setup and the measurement procedure are described elsewhere [17,18], so here it is discussed briefly. A magnetically collimated pulsed electron beam with 200 ns pulse width and 10 kHz repetition rate interacts perpendicularly with an effusive molecular beam produced through a needle of diameter 1 mm. The tip of the needle is kept 4 mm away from the interaction region. Negative ions formed in the interaction region are guided through a spectrometer and collected by a microchannel-plate (MCP) detector. The energy of the emitted electrons is controlled by an external power supply which is connected with the electron gun filament. Filament current is provided by a constant current supply, and the electrons are emitted via a thermionic emission process. The electron-beam current is measured by a Faraday cup, placed opposite to the electron gun in the interaction region. Time-averaged electron-beam current during the measurement was around 3 nA. Two magnetic coils in Helmholtz configuration are used to collimate the electron beam. The typical strength of the magnetic field is 34 Gauss. The axis of the spectrometer is situated perpendicular to both the electron beam and molecular beam. The spectrometer consists of a pusher plate, a puller plate, three lens electrodes, a drift tube, a mesh grid, and a detector. The electron-molecule interaction occurs between the pusher and the puller plate. These pusher and puller plates consist of wire mesh of 90% transmission efficiency to avoid field penetration into the interaction region. After the puller plate, three lens electrodes in Einzel lens configuration are placed to focus the negative ions. The applied voltage to the three electrodes is 90, 1030, and 90 volts, respectively. To increase the mass resolution of the spectrometer, one field-free drift tube is placed after the lens electrodes. At the end of the drift tube, one cap electrode with wire mesh is placed to avoid field penetration into the spectrometer from the detector. Both the drift tube and the cap electrode is biased to 1590 V. After the drift tube, MCP-based detector is placed to collect the negative ions. The detector consists of two MCPs in chevron configuration, along with one collector plate. The time-of-flight (ToF) of the detected ions is determined from the back MCP signal.

The absolute cross section of each fragment anion was measured by using a relative flow technique (RFT) [19–21]. The RFT is basically a calibration procedure where one needs to compare the relative intensities of the species of interest with a standard species of known cross section by keeping the other experimental conditions unchanged. For example, in the present case the absolute cross section of F^- fragment ions from CH_2F_2 is determined by using the dissociative electron attachment (DEA) cross section [22] of O^- ions from O_2 using the equation

$$\sigma(F^-/CH_2F_2) = \sigma(O^-/O_2)\frac{N(F^-)}{N(O^-)}\frac{I_e(O_2)}{I_e(CH_2F_2)} \times \left(\frac{M_{O_2}}{M_{CH_2F_2}}\right)^{1/2}\frac{F_{O_2}}{F_{CH_2F_2}}\frac{K(O^-)}{K(F^-)}. \quad (1)$$

Here, N is the number of fragment ions collected for a fixed time, F is the flow rate of the corresponding gases, I_e is the time-averaged electron-beam current, M is the molecular weight of the parent molecules, K is the detection efficiency, and σ is the absolute cross section. All these factors and their contributions in the overall measurements are discussed in detail in the previous study [17]. Since at low pressure it is very difficult to measure the flow rate accurately, the relative pressure technique (RPT) is also used to determine the absolute cross section. In that case, the above equation takes the form

$$\sigma(F^-/CH_2F_2)=\sigma(O^-/O_2)\frac{N(F^-)}{N(O^-)}\frac{I_e(O_2)}{I_e(CH_2F_2)}\frac{P_{O_2}}{P_{CH_2F_2}}\frac{K(O^-)}{K(F^-)}. \quad (2)$$

The experiment was performed with 99.9% pure commercially available CH_2F_2 gas, and the chamber was kept in ultrahigh vacuum (10^{-9} mbar) for more than one week before the experiment. The mass resolution of the spectrometer is high enough that one can separate the mass difference of 1 amu within this range with the kinetic energy of fragments up to 4 eV [17]. Hence the error due to the impurity is negligible in the measurements. The statistical errors in counting were 5% in the case of F^- and 1% in case of O^-. The procedure for detecting all the other experimental uncertainties involved in the measurements, i.e., electron-beam intensity, flow rate, efficiency of the spectrometer, are discussed in detail in our instrumental paper [17]. Considering all these factors, the overall uncertainty in our measurement is within 15%.

Quantum chemical calculations are performed using the GAUSSIAN 16 software [23]. Thermodynamic threshold energies for each dissociation pathway are obtained from density-functional theory (DFT) using the B3LYP functional [24] and the flexible aug-cc-pVTZ basis set [25]. This level of theory is largely in excellent agreement with experimental results, at least for small molecules [26].

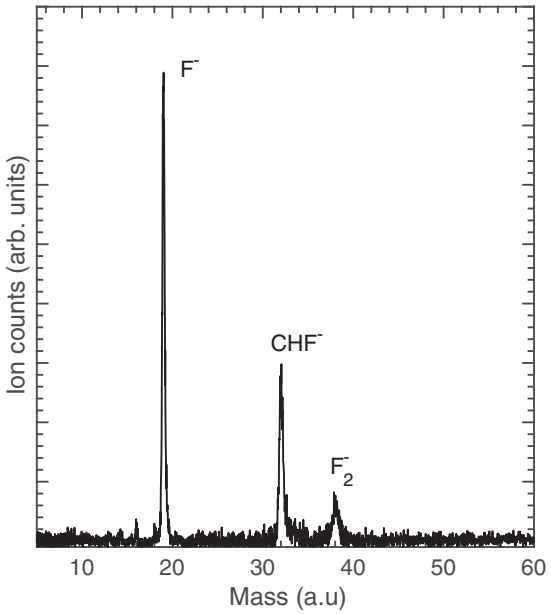

FIG. 2. Mass spectra of the CH_2F_2 at 11 eV incident electron energy after background subtraction. Three different masses F^-, CHF^-, and $F_2{}^-$ are shown, respectively.

III. RESULTS AND DISCUSSION

Within the Franck-Condon (FC) transition window, the resonant capture of low-energy electrons to the ground state CH_2F_2 creates the TNI state of the molecule. After the formation of the TNI, there are two competing channels: One is the dissociation of the TNI by forming a negative ion and neutral conjugates; the other is the autodetachment (AD), where the TNI ejects the electron and goes back to the parent neutral molecule (may be in a vibrationally excited state). Mainly, the lifetime of the TNI determines the cross section or the probability of negative-ion formation. If the lifetime is subsequently sufficiently high (on the order of the vibrational time period of the molecule) that it can cross the critical distance for dissociation, the DEA cross section will be high; otherwise, AD of the TNI dominates. Mass spectra of DEA to CH_2F_2 is recorded from 0 to 15 eV in 1 eV intervals to get insight into the possible dissociation channels. Figure 2 represents the mass spectra of DEA to the CH_2F_2 molecule at 11 eV electron energy, where one can observe three different negative ions: F^-, CHF^-, and $F_2{}^-$. This mass spectra dictates that, in the DEA process, at least three dissociation channels are present. In the previous experimental study, the first two channels (F^- and CHF^-) were observed [15], but the third channel ($F_2{}^-$) is observed for the first time. Ion-yield curve of each fragment anions is recorded from 0 to 16 eV to locate the position of different resonant states involved in the DEA process. Figures 3, 4(a), and 4(b) represent the ion-yield curve of F^-, CHF^-, and $F_2{}^-$ ions, respectively, where one can observe the presence of two resonant states near 2 and 11.4 eV for all three fragment anions. For F^-, a small hump near 9.8 eV followed by a peak near 15.2 eV is also observed. The same behavior was observed previously by Scheuermann *et al.* [15]. In the proceeding sections, the different resonant states and their corresponding dissociation channels are discussed in detail.

A. Resonance at 2 eV

The ion-yield curves of F^-, CHF^-, and $F_2{}^-$ ions [Figs. 3, 4(a) and 4(b)] reveals that the resonant state near 2 eV dissociates by forming three different negative ions. Resonance at such low energy indicates that it is a shape resonance [27]. The

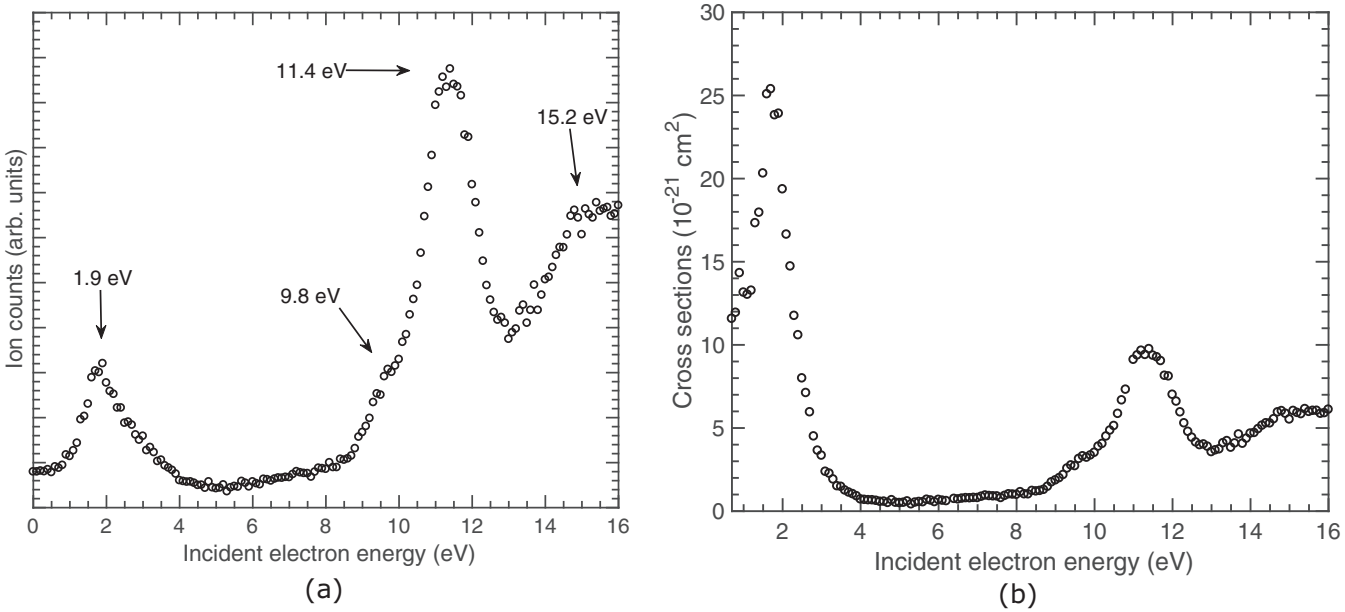

FIG. 3. Ion yield curve of F^- from DEA to CH_2F_2 molecule. (a) The ion-yield curve (without electron-beam intensity correction) up to 16 eV. Three resonance peaks at 1.9, 11.4, and 15.2 eV along with a small hump near 9.8 eV are observed. (b) The electron-beam intensity-corrected cross-section value. Due to low electron-beam current, the cross section below 2.8 eV is suppressed in panel (a). Due to varying electron-beam current, the measured cross-section value is more erroneous in this region.

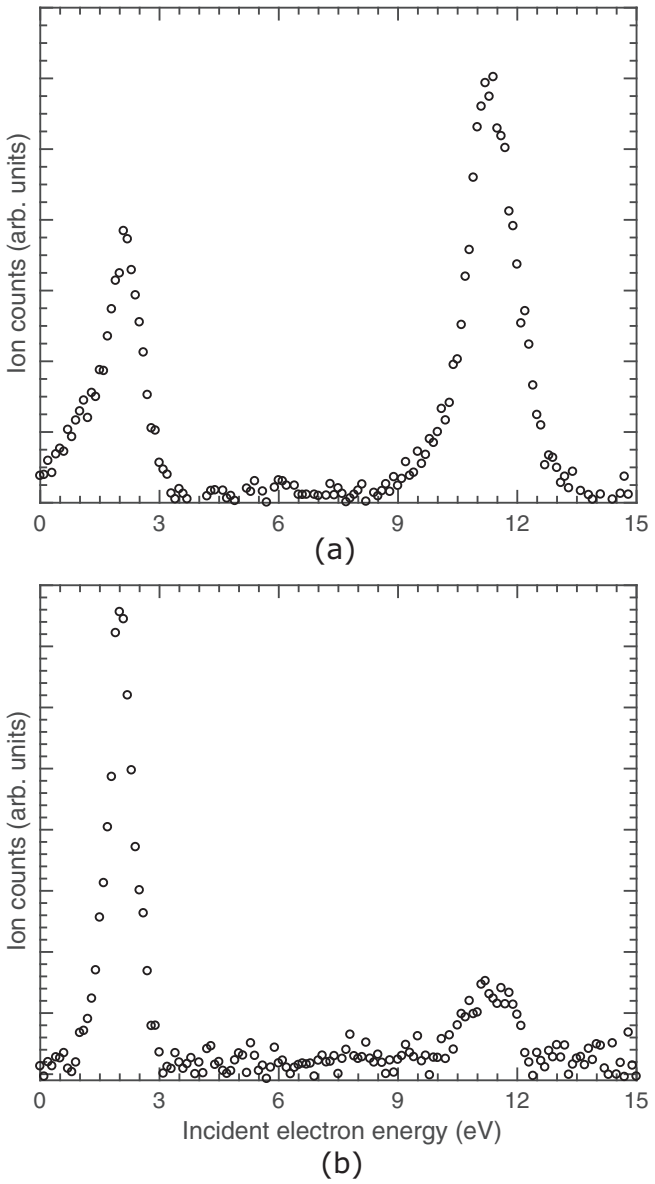

FIG. 4. Ion-yield curves of (a) CHF^- ions and (b) $F_2{}^-$ ions. Two resonance peaks at 2 and 11.4 eV are observed in both cases.

dissociation channels corresponding to the 2 eV resonance are discussed below.

1. F^- *dissociation channel*

Figure 3 represents the ion-yield curve of F^- from DEA to CH_2F_2, where one low-energy resonant state peaking at 1.9 eV is observed. Such low appearance energy indicates that the formation of F^- ion proceeds through the single-bond dissociation of the TNI. The larger cross section of the F^- ion compared with CHF^- and $F_2{}^-$ ions indicates that the TNI dissociates, preferably via the cleavage of a C–F bond. The dissociation channel can be represented as

$$CH_2F_2 + e^- \rightarrow (CH_2F_2)^{-*} \rightarrow F^- + CH_2F. \qquad (3)$$

Our theoretical calculation validates this conclusion further. Table I displays the theoretically calculated threshold energies E_{Th} of different fragment anions resulting from different dissociation channels. The calculated E_{Th} of the F^- ion for the single-bond dissociation process is found to be 1.63 eV. It is relevant to note here that all the ion-yield curves presented in this paper are extremely low-intensity signals. Hence, the accuracy of the AE is estimated to be approximately ± 0.4 eV, i.e., the resolution of our electron gun. One can further derive the thermodynamic threshold of the F^- ion from the thermochemical values available in the literature and compare with our present observation by using the equation

$$K_{\mathrm{F}^-} = \left(1 - \frac{m}{\mathrm{M}}\right)[\mathrm{V}_e - (D - A + E^*)]. \qquad (4)$$

Here, K_{F^-} is the kinetic energy of the F^- ions, m is the mass of the F^- ions, V_e represents the incident electron energy, D represents the bond dissociation energy, A is the electron affinity of F, and E^* is the internal energy of the CH_2F fragment. Now at the threshold energy of this dissociation process, K_{F^-} will be zero. From the literature one can find the bond dissociation energy $D(\mathrm{F\text{-}CH_2F}) = 5.14$ eV [28] and electron affinity $\mathrm{EA(F)} = 3.4$ eV [29]. Now, if the neutral CH_2F molecule formed in the ground state, then by using Eq. (4), the thermodynamic threshold for the formation of the F^- channel is found to be 1.7 eV, which is close to our theoretically obtained threshold energy. This further supports our theoretical calculation and the present experimental result. The measured DEA cross section of the F^- ion at 1.7 eV electron energy is 25.38×10^{-21} cm^2. The time-averaged electron-beam current used in the measurements decreasing continuously below 2.8 eV and reaching to zero at 0 eV [17]. As the electron-beam intensity is directly related to the measured negative-ion counts, the electron-beam intensity-

TABLE I. The experimentally observed appearance energies are compared with the theoretically obtained threshold energies of various dissociation channels. The agreement between these two helped us to identify the proper dissociation channels corresponding to the resonance peak.

Ion	Resonant peak (eV)	Appearance energy (eV)	Dissociation channel	Threshold energy (eV)
F^-	1.9	0.1	$F^- + CH_2F$	1.63
F^-	9.8, 11.4	7.5	$F^- + CHF + H$	6.13
F^-			$F^- + CH_2 + F$	7.47
F^-	15.2		$F^- + CH + H + F$	11.60
F^-			$F^- + CF + H + H$	9.52
CHF^-	11.4	8.5	$CHF^- + H + F$	8.90
$F_2{}^-$	11.2	9.5	$F_2{}^- + CH_2$	6.26

calibrated cross section is shown in Fig. 3(b). If the relative cross section between 1.9 and 11.4 eV peak in Figs. 3(a) and 3(b) is compared, one can observe that the relative cross section below 2.8 eV in Fig. 3(b) is larger than that in Fig. 3(a). At low electron energy where the electron-beam current is very low, the cross section is more erroneous [17].

2. CHF^- and F_2^- dissociation channels

Figures 4(a) and 4(b) represent the ion-yield curve of CHF^- and F_2^- from DEA to the CH_2F_2 molecule. In the recent DEA study of the CH_2F_2 molecule by Gao *et al.*, the authors reported the formation of CHF^- anions from the 11 eV resonance [16]. However, the authors did not report the 2 eV resonance. Previously, in the experimental study by Scheuremann *et al.*, this 2 eV resonance was neglected for extremely low cross section. Due to the total ion collection capability of the newly developed spectrometer, we are able to record the presence of this 2 eV resonant state. The underlying dynamics behind this dissociation process is not as simple as the F^- ion. The formation of CHF^- ions with such low AE indicates that some structural rearrangements occurred in the TNI state. Here a C-H bond dissociates and a H-F bond forms before the final C-F bond dissociation of the TNI state occurred. The dissociation channel of the TNI can be represented as

$$CH_2F_2 + e^- \rightarrow (CH_2F_2)^{-*} \rightarrow CHF^- + HF. \quad (5)$$

Similarly for F_2^- channel, one C–F bond dissociates and a F–F bond forms before the final C–F bond dissociation of the TNI. Structural rearrangements in low-energy TNI states have already been observed in simple biomolecules like CF_2Cl_2 [7] to complex organic acids [30]. To compute the threshold energy for these cases, high level theoretical calculation is required and hence excluded from the present study. The measured cross-section values of these two ions are too low to report any reliable absolute value, hence the differential values are reported only.

B. Resonances around 11.4 eV

In the measured excitation function of the three negative ions [Figs. 3, 4(a), and 4(b)], one broad resonance peak near 11.4 eV is observed. Along with the 11.4 eV resonance peak, one small hump near 9.8 eV and another resonance peak around 15.2 eV is also observed for the F^- anion (Fig. 3). The presence of 9.8 and 15.2 eV resonant states along with 11.4 eV was observed previously [15]. This indicates the presence of more than one closely lying resonant state in the Franck-Condon transition region. To understand this behavior, results are compared with the previous experimental and theoretical studies [6,10]. Using electron transmission spectroscopy (ETS) and multiple scattering Xα (MS-Xα) bound-state calculations; Modelli *et al.* studied the electron attachment to halomethanes [6]. Here, the authors made a detailed comparison between the experimentally observed electron attachment cross sections with the theoretically obtained values for the halomethane compounds. They obtained a nice agreement between the theoretically and experimentally observed values, which confirms the reliability of their theoretical calculations. Due to the unavailability of the sample, they could not perform any experimental study for the CH_2F_2 molecule; however, their theoretical observations indicate that two broad σ^* resonant states with symmetry B_2 and A_1 with comparable intensities are present around 10 eV. The same conclusion was drawn by Varella *et al.*, where the authors performed complete theoretical and experimental differential cross-section measurement studies of the CH_2F_2 molecule [10]. Here, the authors indicate the presence of two resonant states at 10.5 eV ($^2A_1$) and 11.5 eV ($^2B_2$) [10]. Recently Gao *et al.* reconfirmed the presence of an 11 eV resonant state in CH_2F_2. Comparing with the previous studies, in the present case, a clear signature of the resonant states around these above-mentioned energy ranges are observed. Two peaks, as mentioned by Modelli *et al.* and Varella *et al.*, are not possible to observe separately due to poor electron gun resolution; however, a small hump at 9.8 eV along with a clear peak at 11.4 eV is observed in the F^- ion yield. The presence of 15.2 eV resonant state in the ion yield of F^- ions is beyond the present understanding, although its presence was recorded previously [15].

1. F^- dissociation channel

A resonance that occurred at such high energy (generally above the first excitation energy of the molecule) can be associated with the core excited Feshbach resonance, where the resonant electron capture occurred in one of the metastable valance states of the molecule [27]. To identify the proper dissociation channel corresponding to these resonant states, threshold energies are calculated and compared with the experimentally observed appearance energy (AE). Such a high AE clearly dictates that this resonant state dissociates through a multibond dissociation process forming F^- ions. The dissociation channels can be represented as

$$CH_2F_2 + e^- \rightarrow (CH_2F_2)^{-*} \rightarrow \begin{cases} F^- + CHF + H\ (a) \\ F^- + CH_2 + F\ (b) \\ F^- + CH + H + F\ (c) \\ F^- + CF + H + H\ (d). \end{cases} \quad (6)$$

Calculated threshold energies corresponding to each dissociation channels are listed in Table I. Reactions (6)(a) and (6)(b) are the two bond dissociation processes with threshold energies 6.13 and 7.47 eV, respectively. This certainly indicates that the resonant states at 9.8 and 11.4 eV are associated with these two dissociation channels. For reactions (6)(c) and (6)(d), the calculated threshold energies are 11.6 and 9.52 eV, respectively, indicating the possible involvement of the three-body dissociation process for the 15.2 eV resonant state. It is to be mentioned here that high AE energy does not always indicate a multibond dissociation process. Sometimes the excess energy is absorbed by the dissociating fragments, resulting in their excited states. In the present study, the dissociation channels are predicted only by looking at the corresponding threshold energies. The measured absolute DEA cross section of the F^- ions at 11.4 eV is 9.75×10^{-21} cm^2.

Upon close inspection of Fig. 3(a), one can observe that the cross section of the F^- ion is gradually increasing beyond 8 eV incident electron energy. Continuous increase in ion counts with increasing electron energy indicates the involvement of an ion-pair dissociation (IPD) process around

this energy [31]. The same behavior was observed previously by Scheuremann *et al.* [15]. Recently Gao *et al.* [16] found that the threshold energy of CHF^- ions for the ion-pair dissociation process of CH_2F_2 is around 18.67 eV. However, the authors did not mention anything about the F^- ions. The only two experimental observations of the F^- ion-yield curve indicates the possible involvement of ion-pair states around 8 eV; this means, in the FC transition window, the ion-pair state lies below the TNI state, and at 11.4 eV, DEA and IPD processes coincide [15]. Hence, in the FC transition window, more than one TNI and ion-pair states could be possible in this energy region. This observation is purely speculative at the moment and drawn by observing the nature of the ion-yield curve only. A high-level theoretical calculation is required to further understand this behavior.

2. CHF^- *and* F_2^- *dissociation channels*

Figure 4(a) represents the ion-yield curve of CHF^- where a resonance peak at 11.4 eV is observed. The same behavior was found in previous experimental studies [15,16]. Resonance at such high energy indicates the involvement of a core excited Feshbach resonance [27]. In the present context, a theoretical threshold energy calculation is performed in order to identify the proper dissociation channels. Such high AE of the CHF^- anions indicates that a two-bond dissociation process is involved. The dissociation channel can be represented as

$$CH_2F_2 + e^- \rightarrow (CH_2F_2)^{-*} \rightarrow CHF^- + H + F. \quad (7)$$

The calculated threshold energy of the above-mentioned reaction channel is 8.9, which is close to the experimentally obtained AE (Table I). In the recent study, Gao *et al.* discussed the different dissociation channels of the TNI state, forming CHF^- anions [16]. The authors indicate the involvement of concerted dissociation process, as mentioned in Eq. (7).

For F_2^- ions, a small resonance peak can be observed near 11.2 eV [Fig. 4(b)]. As mentioned earlier, one possibility of the F_2^- dissociation channel is through the structural rearrangements in the TNI state. A further experimental and theoretical investigation is required to understand the dynamics of this dissociation process and is daring to comment on anything based on the present understanding. However, one can try to find some similarities with the recently documented DEA studies of the SO_2 molecule [32,33]. According to Gope *et al.* [33], the S^- dissociation channel proceeds while producing the O_2 molecule as the neutral conjugate. This dissociation process requires the two vibrational modes' simultaneous occurrence: symmetric stretching and symmetric bending of the SO_2 molecule. Dissociation of two S–O bonds along with the formation of an O–O bond occurred in this process. Similarly, in the case of CH_2F_2, one can think of two C–F bond dissociations along with the formation of a F–F bond for the F_2^- dissociation channel. The dissociation channel could be represented as

$$CH_2F_2 + e^- \rightarrow (CH_2F_2)^{-*} \rightarrow F_2^- + CH_2. \quad (8)$$

The calculated threshold energy of this dissociation channel is found to be 6.26 eV. The large difference between the threshold energy and the AE [Fig. 4(b)] indicates that the fragments are formed in their corresponding electronic excited states. In the case of DEA to the SO_2 molecule [33], a similar thing is observed. However, it is purely speculative at the moment and needs more studies to understand the process properly. Due to extremely low counts, we are unable to report any meaningful absolute cross-section value for CHF^- and F_2^-.

IV. CONCLUSION

The absolute cross section of F^- ions from DEA to CH_2F_2 has been measured within 0 to 16 eV electron energy range by using the relative flow technique. One low-energy resonant peak near 2 eV followed by two higher-energy peaks near 11.4 and 15.2 eV have been observed. One small hump near 9.8 eV is also observed. Three different negative ions, F^-, CHF^-, and F_2^- are observed as dissociation products of all the resonant states. The presence of the F_2^- ion in the DEA to CH_2F_2 is observed. Theoretical threshold-energy calculations helped us to assign the proper dissociation channel corresponding to each resonant state. From the ion-yield curve of the F^- ion, we speculate that around 11.4 eV electron energy, the DEA and IPD processes coincide. The absolute DEA cross section of the F^- ion is reported. The experimental result indicates that more than one different TNI and IP states of the CH_2F_2 molecule are available within 0 to 16 eV energy range. Detailed experimental and theoretical studies in this direction are further required to understand the dynamics properly.

ACKNOWLEDGMENTS

D.N. gratefully acknowledges the partial financial support from "Indian National Science Academy (INSA)" under Project No. "SP/YSP/80/2013/734" and from the "Science and Engineering Research Board (SERB)" under Project No. "EMR/2014/000457." D.C. acknowledges IISER Kolkata for providing a Ph.D. research fellowship and the Center for Research Computing at the University of Notre Dame for providing the computational facilities. D.C. also acknowledges Notre Dame Radiation Laboratory, which is supported by the US Department of Energy under award DE-FC02-04ER15533.

[1] L. G. Christophorou, J. K. Olthoff, and M. V. V. S. Rao, J. Phys. Chem. Ref. Data **25**, 1341 (1996).

[2] E. Illenberger and J. Momigny, *Gaseous Molecular Ions: An Introduction to Elementary Processes Induced by Ionization*, Topics in Physical Chemistry (Steinkopff, 2013).

[3] M. Stano, V. Foltin, S. Matejcik, J. Langer, S. Gohlke, and E. Illenberger, J. Phys. B: At., Mol. Opt. Phys. **36**, 443 (2003).

[4] P. Rawat, V. S. Prabhudesai, M. Rahman, N. B. Ram, and E. Krishnakumar, Int. J. Mass Spectrom. **277**, 96 (2008).

[5] J. H. Moore, P. Swiderek, S. Matejcik, and M. Allan, *Nanofabrication Using Focused Ion and Electron Beams* (Oxford University Press, Oxford, 2012), Chap. 4.

[6] A. Modelli, F. Scagnolari, G. Distefano, D. Jones, and M. Guerra, J. Chem. Phys. **96**, 2061 (1992).

[7] J. Langer, S. Matt, M. Meinke, P. Tegeder, A. Stamatovic, and E. Illenberger, J. Chem. Phys. **113**, 11063 (2000).
[8] C. R. Brundle, M. B. Robin, and H. Basch, J. Chem. Phys. **53**, 2196 (1970).
[9] H. Tanaka, T. Masai, M. Kimura, T. Nishimura, and Y. Itikawa, Phys. Rev. A **56**, R3338 (1997).
[10] M. T. do N. Varella, C. Winstead, V. McKoy, M. Kitajima, and H. Tanaka, Phys. Rev. A **65**, 022702 (2002).
[11] T. Nishimura, J. Phys. B: At., Mol. Opt. Phys. **31**, 3471 (1998).
[12] D. Chakraborty and D. Nandi, arXiv:1806.09352.
[13] S. Motlagh and J. H. Moore, J. Chem. Phys. **109**, 432 (1998).
[14] I. Torres, R. Martínez, M. N. S. Rayo, and F. Castaño, J. Phys. B: At., Mol. Opt. Phys. **33**, 3615 (2000).
[15] H.-U. Scheunemann, M. Heni, E. Illenberger, and H. Baumgärtel, Ber. Bunsen-Ges. Phys. Chem. **86**, 321 (1982).
[16] X.-F. Gao, H. Li, X. Meng, J.-C. Xie, and S. X. Tian, J. Chem. Phys. **152**, 084305 (2020).
[17] D. Chakraborty, P. Nag, and D. Nandi, Rev. Sci. Instrum. **89**, 025115 (2018).
[18] D. Chakraborty, Ph.D. thesis, Indian Institute of Science Education and Research, Kolkata, 2019 (unpublished).
[19] E. Krishnakumar and S. K. Srivastava, J. Phys. B: At., Mol. Opt. Phys. **21**, 1055 (1988).
[20] O. J. Orient and S. K. Srivastava, J. Chem. Phys. **78**, 2949 (1983).
[21] S. K. Srivastava, A. Chutjian, and S. Trajmar, J. Chem. Phys. **63**, 2659 (1975).
[22] D. Rapp and D. D. Briglia, J. Chem. Phys. **43**, 1480 (1965).
[23] M. J. Frisch, G. W. Trucks, H. B. Schlegel, G. E. Scuseria, M. A. Robb, J. R. Cheeseman, G. Scalmani, V. Barone, B. Mennucci, G. A. Petersson, H. Nakatsuji, M. Caricato, X. Li, H. P. Hratchian, A. F. Izmaylov, J. Bloino, G. Zheng, J. L. Sonnenberg, M. Hada, M. Ehara *et al.*, *Gaussian 09 Revision E.01* (Gaussian Inc. Wallingford, Connecticut, USA, 2009).
[24] A. D. Becke, J. Chem. Phys. **98**, 5648 (1993).
[25] T. H. Dunning, J. Chem. Phys. **90**, 1007 (1989).
[26] M. Zawadzki, P. Wierzbicka, and J. Kopyra, J. Chem. Phys. **152**, 174304 (2020).
[27] G. J. Schulz, Rev. Mod. Phys. **45**, 423 (1973).
[28] J. Shi, J. He, and H.-J. Wang, J. Phys. Org. Chem. **24**, 65 (2011).
[29] C. Blondel, C. Delsart, and F. Goldfarb, J. Phys. B: At., Mol. Opt. Phys. **34**, L281 (2001).
[30] S. Pshenichnyuk and N. L. Asfandiarov, Phys. Chem. Chem. Phys. **22**, 16150 (2020).
[31] D. Chakraborty, P. Nag, and D. Nandi, Phys. Chem. Chem. Phys. **18**, 32973 (2016).
[32] I. Jana and D. Nandi, J. Phys. B: At., Mol. Opt. Phys. **52**, 185202 (2019).
[33] K. Gope, V. S. Prabhudesai, N. J. Mason, and E. Krishnakumar, J. Chem. Phys. **147**, 054304 (2017).